Ecological patterns of benthic foraminiferal communities driven by seasonal and spatial environmental gradients in an Arctic fjord

Corentin Guilhermic, Maria Pia Nardelli, Aurélia Mouret, Antonio Pusceddu, Agnès Baltzer, Hélène Howa

LIMNOLOGY and OCEANOGRAPHY

ASLO

Limnol. Oceanogr. 9999, 2024, 1–14

doi: 10.1002/lno.12691

Ecological patterns of benthic foraminiferal communities driven by seasonal and spatial environmental gradients in an Arctic fjord

Corentin Guilhermic,[1*] **Maria Pia Nardelli**,[1] **Aurélia Mouret**,[1] **Antonio Pusceddu**,[2] **Agnès Baltzer**,[3] **Hélène Howa**[1]

[1]Nantes Université, Le Mans Université, CNRS, Laboratoire de Planétologie et Géosciences, University of Angers, Angers, France
[2]Department of Life and Environmental Sciences, University of Cagliari, Cagliari, Italy
[3]LETG, UMR CNRS 6554, University of Nantes, Nantes, France

Abstract

Arctic fjords, being transitional areas between glacier-covered land and the ocean, are characterized by strong environmental gradients. The seasonal melting of glaciers generates strong turbidity and primary production antagonist gradients, which can affect benthic habitats. Two sampling campaigns were carried out in Kongsfjorden (Svalbard, Arctic Ocean) in May and August 2021 to investigate seasonal changes in benthic foraminifera spatial distribution and ecosystem functioning along a longitudinal transect of 10 km from the Kronebreen tidewater glacier front. Concurrently, organic matter quantity and biochemical composition, sediment grain size, and physical parameters of the water masses were investigated as possible driving factors of benthic ecosystem responses. In a previous study, three statistically determined foraminiferal biozonations (glacier proximal, medial, and distal) were observed on the basis of their species content within the closest 10 km from the glacier front, presenting similar assemblages in both seasons. Our results indicate that foraminiferal distribution at the local scale is mainly driven by physical and geochemical gradients induced by melting waters and sediment discharges from the tidewater glacier occurring during summer. Due to the climate change, the melting season is expected to last longer and increasing global temperature will much probably accelerate the melting processes. Our findings strongly support the use of foraminifera as bioindicators to monitor the effects of ongoing climate change on the benthic ecosystems of Arctic fjords and, accessorily, as proxies for reconstructing glacier front positions in the recent past.

Arctic regions are undergoing changes in all their environmental components, including ocean, cryosphere, and atmosphere, due to global warming and ecosystems have reached hard adaptation limits (IPCC 2023). Between 1979 and 2018, global sea surface temperature increased by up to 0.5°C per decade, while sea ice concentration decreased by 12% per decade in summer in the Arctic (Perovich and Richter-Menge 2009; IPCC 2022). Differently from other parts of the world, Arctic regions experience the so-called polar amplification, which has caused surface air temperature to double compared to the global average over the past two decades (Richter et al. 2012; Notz and Stroeve 2016). The northward rise in temperature is favored by the delayed freeze-up of sea-ice and the progressive warming of Arctic water masses (Lind et al. 2018). This phenomenon is particularly noticeable on the western Svalbard continental shelf (74–81°N and 10–35°E), where warm Atlantic water (AW) has become more present during the year since the early 2000s due to weakened southward advection of cold Arctic water (ArW) (Lind et al. 2018; Strzelewicz et al. 2022). Altering the balance between cold and warm water masses intrusions affects the local hydrography of the fjords located on the western coast of Spitsbergen, which in turn influences their seasonal and interannual variability (Svendsen et al. 2002; Cottier et al. 2005; Payne and Roesler 2019).

The seasonal dynamics of these marine intrusions combined with the down-fjord flow of cold meltwaters, generates extremely strong environmental gradients. The yearly cycle

*Correspondence: cguilhermic@gmail.com

Additional Supporting Information may be found in the online version of this article.

Author Contribution Statement: CG: conceptualization, data curation, formal analysis, investigation, methodology, visualization, writing-original draft, writing-review and editing. MPN: conceptualization, funding acquisition, investigation, resources, supervision, validation, writing-review and editing. HH and AM: conceptualization, investigation, supervision, validation, writing-review and editing. AP: methodology, investigation, data curation, formal analysis. AB: funding acquisition.

beginning with the establishment of a cold homogeneous water column in late fall/early winter due to a drop in atmospheric temperature and no sunlight (Cottier et al. 2005) rapidly changes during spring. Indeed, the increase of solar radiation and atmospheric temperatures triggers phytoplanktonic bloom followed by a stratification of the water column with the intrusion of warm and salty Atlantic water bodies (Svendsen et al. 2002; Payne and Roesler 2019). The warming of the overall water column added to the increase in atmospheric temperature both contribute to the melting of marine terminating glaciers. This brings freshwater at the surface of the fjord accompanied with large nutrient and sediment supplies increasing the turbidity hampering phytoplanktonic growth in the vicinity of the glacier's fronts (e.g., van De Poll et al. 2016; Hegseth et al. 2019). As fjord ecosystems, from the pelagic to the benthic realms, are highly sensitive to hydrographic variations on a seasonal scale (Hop and Wiencke 2019), climate change is expected to have strong consequences for Arctic coastal ecosystems.

The present study addresses the benthic ecosystems of Kongsfjorden, where large seasonal variations in benthic community structure are expected in response to strong seasonality of local environmental drivers, such as water mass circulation and stratification, sediment discharges, primary production. Nonetheless, while several studies reported seasonal phytoplanktonic dynamics in Kongsfjorden (Hegseth et al. 2019; Hop and Wiencke 2019; Hoppe 2022), little is known about seasonal dynamics of benthic ecosystems in the area under scrutiny. In this regard, while inconsistent signals of seasonal variability in macrofaunal and meiofaunal communities have been reported in Kongsfjorden, benthic foraminiferal communities could exhibit clear seasonal patterns (Włodarska-Kowalczuk et al. 2016). Indeed, foraminifera are known for their ability to keep pace with rapid changes in the environment due to their short life cycle and species ecological requirements (Jorissen et al. 1995; Bouchet et al. 2018). As a result, they can be used to monitor fast environmental changes (e.g., Richirt et al. 2020; Jorissen et al. 2022). Previous studies investigated foraminifera in different regions of Svalbard to characterize past (Husum et al. 2019) or modern environments (Jernas et al. 2018; Fossile et al. 2020; Jima et al. 2022). In the middle to outer Kongsfjorden, changes in benthic foraminiferal communities were related to the progressive atlantification of the fjord (Jernas et al. 2018). In the innermost part of the fjord, within 10 km from the Kronebreen glacier, Fossile et al. (2022) showed that during the melting season, sediment instability was associated to low organic production within the turbid plume derived from the glacier. It sensibly influences foraminiferal distribution according to the study.

The present study focuses on seasonal changes in benthic foraminiferal distribution and faunal composition during two periods of a same year: spring (May) and late summer (August) 2021. Foraminiferal vertical distribution in the sediment column was investigated, along with environmental parameters such as organic matter quantity and biochemical composition, sediment grain size, and water column physical parameters. As the warm season tends to settle extensively in the fjord throughout years due to global warming (Divya and Krishnan 2017; Hop and Wiencke 2019), interseasonal response of benthic foraminifera to varying environmental gradients in Kongsfjorden was studied with the aims of understanding the present-day functioning of these ecosystems. It results in providing predictions about the consequences of drastic changes in seasonality expected due to climate change on benthic foraminiferal biodiversity and ecosystem functioning.

Materials and methods

Study area

Kongsfjorden is a high-latitude fjord (79°N, 12°E) located on the western coast of Spitsbergen, the largest island in the Svalbard archipelago (Fig. 1). A shallow inner sill, located near the Lovénøyane islands, partially isolates the fjord head (Fig. 1, about 20 m water depth) (Howe et al. 2003; Halbach et al. 2019).

Kongsfjorden contains both land-terminating and marine-terminating glaciers (or tidewater glaciers) at its head (Dallmann 2015). Five tidewater glaciers flow into Kongsfjorden: Blomstrandbreen, Conwaybreen, Kongsbreen, Kronebreen, and Kongsvegen (Fig. 1). The last two share the same terminus between the southern coast and the Colletthøgda formation at fjord head (Fig. 1; Halbach et al. 2019). Sediment discharge mostly originates from tidewater glacier creep and subglacial rivers that deliver detrital products from different areas of the catchment to the fjord resulting from summer precipitations, high atmospheric temperature, and frontal calving. Depending on the glacier watersheds, erosion of the various basal rocks results in the input of siliciclastic and/or carbonate particles into the fjord (Dallmann 2015; D'Angelo et al. 2018).

As a subpolar fjord (Howe et al. 2010), Kongsfjorden used to be considerably covered by sea-ice in winter until 2006 (Payne and Roesler 2019; Tverberg et al. 2019). But sea-ice extension rapidly decreased over the last decade and only patchy sea-ice cover is observed at present, mostly near the northern coast of the fjord. This phenomenon was linked to the progressive atlantification of the Fram strait (Lind et al. 2018; Strzelewicz et al. 2022) and the associated warmer water masses intruding the fjord during summer (Divya and Krishnan 2017).

Environmental parameters

Conductivity–temperature–depth profiles

During the two sampling campaigns, in spring and summer 2021, conductivity–temperature–depth (CTD) casts were performed at the four stations shown in Fig. 1. Water column measurements were performed using a CTD profiler (SAIV

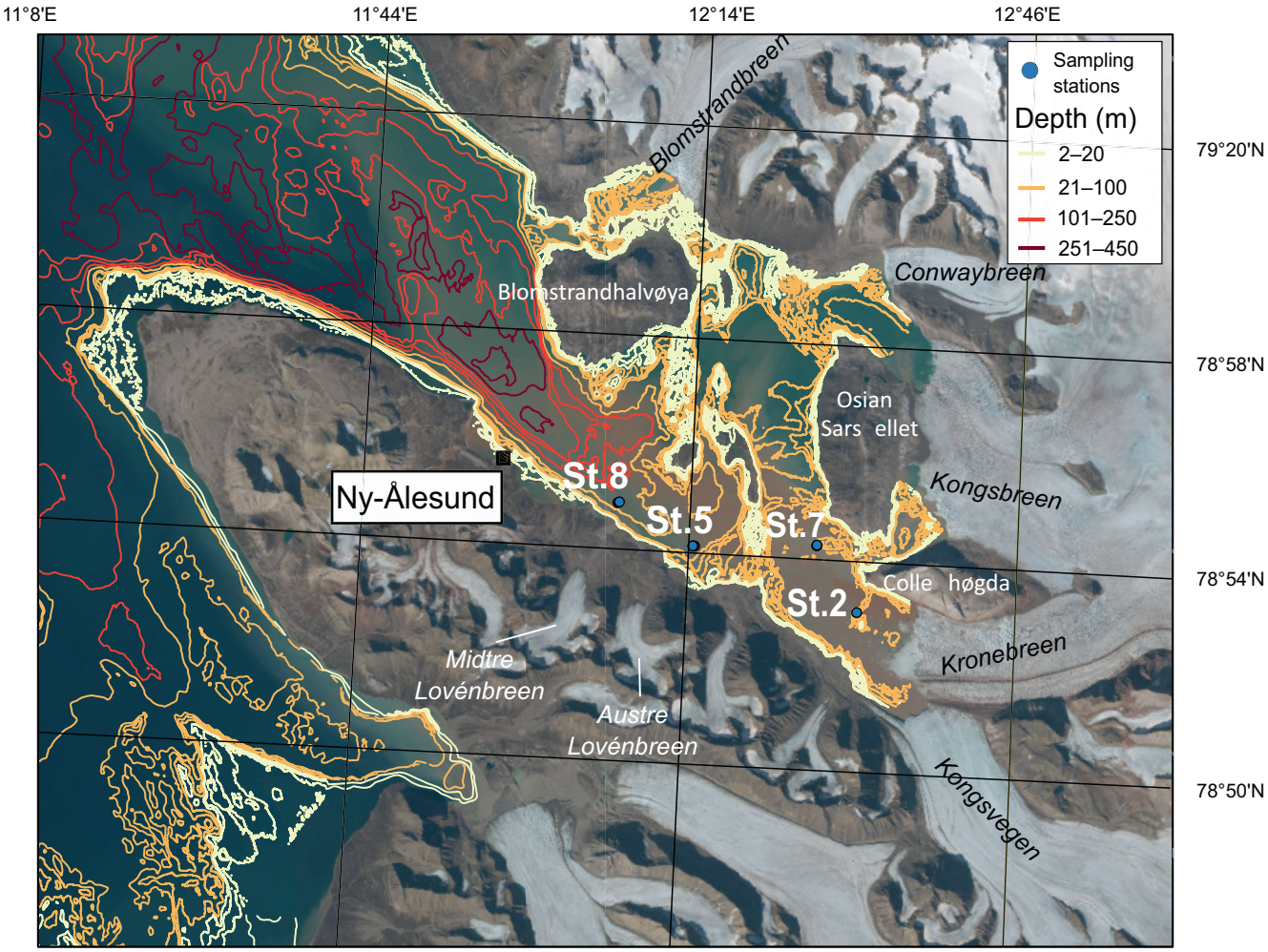

Fig. 1. Map of Kongsfjorden displaying the location of the four studied stations (tidewater glaciers in black letters). Bathymetric data are symbolized by yellow to dark red lines associated with different depth ranges (*see* legend). Data from the Norwegian Hydrographic Service (Karverket). Satellite image was extracted from TopoSvalbard.npolar.no (NorskPolar Institutt) and was taken in July/August 2020.

SD204). Section profiles were plotted using Ocean Data View software 5.6.2 (Schlitzer 2023). Spatial interpolation between profiles was performed using ODV in-built DIVA tool (data interpolating variational analysis) (Iona et al. 2018).

Sediment sampling. Sediment samples were collected in Kongsfjorden in spring (26 April 2021–2110 May 2021), and in summer (16 August 2021–2030 August 2021). We sampled the same stations (Table S1) as Fossile et al. (2022) as part of an annual monitoring program of the inner fjord area influenced by sediment discharges from Kronebreen glacier (BEGIN/KONBHAS projects). Coring was performed on the R/V *Teisten* (King's Bay) using two devices, depending on the texture of the sediment, both allowing to sample the sediment–water interface with minimum disturbance: GEMAX gravity corer for unconsolidated silt and Day Grab (1000 cm^2; K/C Demark A/S) for coarser bottom. The GEMAX corer was used to recover twin cores (9 cm inner diameter). Subsampled cores (8.2 cm inner diameter) were collected from the top of the Day Grab (up to 10 cm long). This device is equipped of four top windows allowing the susbsampling of undisturbed sediment without opening the grab (Fig. S1).

At each station, one core was retrieved for foraminifera, one for grain size and three others for organic matter. The collected cores were sliced on land after sampling. Sediment layers for all analyses were recovered with the same slicing resolution: every 0.5 cm until 2 cm depth, 1 cm thick slices from 2 to 10 cm depth.

Grain-size analysis. For grain-size analyses, samples were cool-stored at 4°C (spring mission) or freeze-dried and rehydrated before the analyses (summer mission). An aliquot (~ 0.1 g) was analyzed by a Malvern Mastersizer 3000 laser diffraction particle analyzer. Data were processed with GRADISTAT 9.0 software (Blott and Pye 2001). The obtained

modes (Fig. S2) were used as potential environmental driver compiled in statistical analyses (RDA).

Organic matter sedimentary contents and biochemical composition. For organic matter analyses, topmost sediment layer (0–0.5 cm) from each of the retrieved cores was frozen at − 20°C until analysis. Sediments were then analyzed for total protein, carbohydrate, lipid, and phytopigment contents on two to three measurements per core. Phytopigments sedimentary content (in terms of chlorophyll *a* [Chl *a*] and phaeopigments) was fluorometrically analyzed according to Lorenzen and Jeffrey (1980), after extraction with 9% acetone. A conversion factor of 30 $\mu g\,\mu g^{-1}$ was applied to obtain C equivalents (Pusceddu et al. 2010).

Total protein, carbohydrate, and lipid (BPC; biopolymeric carbon components) were analyzed by spectrophotometry following the protocols detailed in Danovaro (2009). Results were respectively converted into C equivalents using the following conversion factors: 0.49, 0.40, and 0.75 mg C mg^{-1}, and their sum reported as the biopolymeric carbon (Fabiano et al. 1995). The algal fraction of BPC, a proxy for the nutritional quality of biopolymeric C (Pusceddu et al. 2010), was estimated as the percentage ratio of total phytopigment and biopolymeric C contents. Extracellular protein potential degradation rates and turnover (aminopeptidase) were analyzed as a main indicator of local ecosystem functioning. For detailed protocol, *see* Supporting Information.

Living benthic foraminifera processing

Sample processing. After sampling, foraminiferal samples were stored in a solution of 2 g L^{-1} Rose Bengal in 95% ethanol. Samples were sieved at 63 and 125 μm. All Rose Bengal–stained benthic foraminifera were wet-picked for the > 125 μm size fraction under stereomicroscope. Species were considered minor if they counted for less than 5% of the assemblages. The large tubular agglutinated species *Archimerismus subnodosus* was only included in species richness calculations but not in abundance calculations because of its important fragmentation in the samples. All graphical representations were performed using GRAPHER® 16.2.354 (Golden Software).

Diversity metrics and statistical analysis. Species richness (*S*) was determined as the number of species identified in the assemblages. The Shannon index (*H'*) and Piélou evenness (*J*) were additionally calculated using EXCEL.

A transformation-based redundancy analysis (tb-RDA) was performed to identify which among the measured environmental variables mostly influenced foraminiferal abundances (0–5 cm and > 125 μm). Significant environmental variables tested in the RDA were previously identified by the function *anova.cca* from the R package *vegan* (Oksanen 2015). Hellinger transformation was applied to foraminiferal abundances and environmental variables using the *decostand* function. The final tb-RDA was performed in R software using the *vegan* package (Oksanen 2015).

Results

Environmental context

Water masses data

In May, the casts from all stations showed a well-mixed water column along the entire transect with only slight variations in salinity (< 0.1) and cold temperatures, varying from 0.6°C at the bottom to a minimum of − 1.5°C at the surface (Fig. 2). The coldest surface temperatures were recorded at the two stations closest to the Kronebreen glacier front (Stas. 7 and 2). Turbidity was very low (< 10 FTU) and Chl *a* concentration was always below 0.4 $\mu g\,L^{-1}$. This maximum pigment concentration was observed at Stas. 5 and 8, between 10 and 40 m water depth (Fig. 2).

At the opposite, at the end of August, the water column was well stratified at all stations, with fresher (< 33) and cooler (< 4°C) water within the top 10 m (Fig. 2). Near the seafloor, salinities varied from 34.75 at Sta. 8 to values between 34.6 and 34.25 at Stas. 5, 2, and 7. Temperature was below 3°C at Sta. 8, while it remained between 3°C and 4.5°C at Stas. 5, 2, and 7. A steep gradient along the transect was observed for turbidity and Chl *a* concentration in the surface water (SW). Indeed, a well-defined turbidity peak marked the presence of a turbid plume between 5 and 20 m depth at Sta. 2, close to the glacier terminus, which rapidly decreased toward the distal stations. Inversely, Chl *a* peak concentration started at the fringe of the turbid plume from Sta. 7 to distal ones.

Sediment data

Organic matter quantity and biochemical composition. Biopolymeric C (BPC) sedimentary contents (Fig. 3a) varied were 1.23 ± 0.33 mg g^{-1} C in May and 1.23 ± 0.30 mg g^{-1} C in August. The BPC sedimentary contents at the two distal stations (5 and 8) were significantly higher (ANOVA, $p = 0.02$) than in the two other glacier proximal stations and did not vary between seasons (ANOVA, $p = 0.99$) (Supporting Information). Total phytopigment concentrations in surface sediment (Fig. 3b) ranged from 0.80 ± 0.03 and 11.63 ± 0.25 $\mu g\,g^{-1}$ in May to 1.24 ± 0.17 and 15.92 ± 6.85 $\mu g\,g^{-1}$ in August. Highest concentrations were found in the glacial distal Stas. 5 and 8 with differences between May and August values. Both in May and August, the algal fraction of BPC (Fig. 3c) at Sta. 5 (0.18 and 0.45 ± 0.11) and Sta. 8 (0.27 ± 0.04 and 0.19 ± 0.03) was higher than that at Sta. 2 (0.05 for summer) and Sta. 7 (0.04 and 0.09 ± 0.02). Strong and significant seasonal differences in the algal fraction of BPC occurred only at Stas. 5 and 7, where values in August were more than twice those in May. Aminopeptidase activity used to assess extracellular protein degradation rates, was significantly lower (ANOVA, $p = 0.03$) (Fig. 3d) at the proximal Stas. 2 and 7 compared to

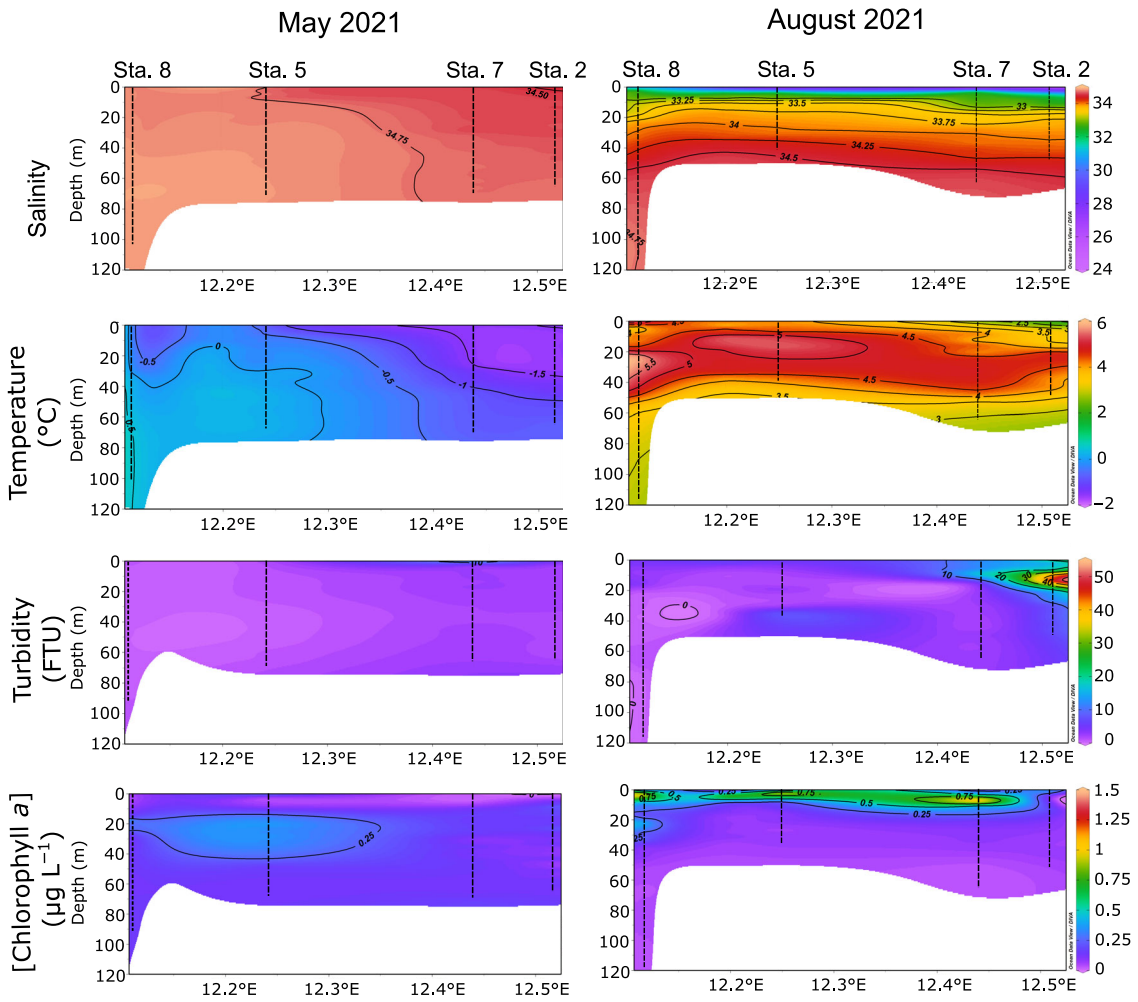

Fig. 2. Sections across the deep transect (0–120 m water depth) of interpolated (DIVA interpolation) profiles for salinity, temperature, chlorophyll *a* concentration, and turbidity (FTU, "formazine turbidity unit"). Sampling station locations are marked by dotted lines. Sections on the left column are May 2021 data and the sections on the right are August 2021 data. Color scales are different for each parameter but common for one parameter between seasons.

the glacier the distal Stas. 5 and 8. It exhibited significant seasonal changes only at Sta. 7, where values in August (5.53 ± 0.47 and 18.39 ± 4.83 nmol g^{-1} h^{-1}) were higher than those in May.

Foraminiferal diversities and abundances. Foraminiferal abundances and diversity metrics for the whole top 0–5 cm sediment interval are presented in Fig. 4 for both spring and summer. In both seasons, foraminiferal abundances increased from the glacier front area (Sta. 2) to the distal zone (Sta. 8). Abundances were much lower in spring than in summer at all stations (0 and 463 ind. 50 cm^{-2} for Sta. 2, 13 and 803 ind. 50 cm^{-2} for Sta. 7, 1155 and 1963 ind. 50 cm^{-2} for Sta. 5, and 1727 and 2196 ind. 50 cm^{-2} for Sta. 8, in May and August, respectively). The species richness (*S*) (Fig. 4b) was lower at the proximal Stas. 2 and 7, with 0–7 species, respectively, compared to the medial station Sta. 5, with 30–33 species, and the distal station Sta. 8, with 23–28 species. The highest diversity values were observed at the medial station Sta. 5 in both spring and summer. The number of species found at each station in spring and summer varied only with a maximum difference of five species at Sta. 8. All species richness remained similar between seasons, with a maximum change in Sta. 8 in which was observed an increase of five species in summer.

In August 2021, the lowest Shannon index ($H' = 0.1$) was measured at Sta. 2. At Sta. 7, H' was 1.1 in spring and 0.5 in summer. At Stas. 8 and 5, H' was > 2 in both seasons, with a difference of less than 0.5 between seasons (Fig. 4c). Equitability (*J*) values at Sta. 2 were below 0.1 in summer 2021 and did not vary with season at Stas. 8 and 5, ranging between 0.59 (Sta. 5, summer) and 0.71 (Sta. 8, summer) (Fig. 4d).

The analysis of the relationships between species richness (*S*) and aminopeptidase activity (as a proxy for ecosystem

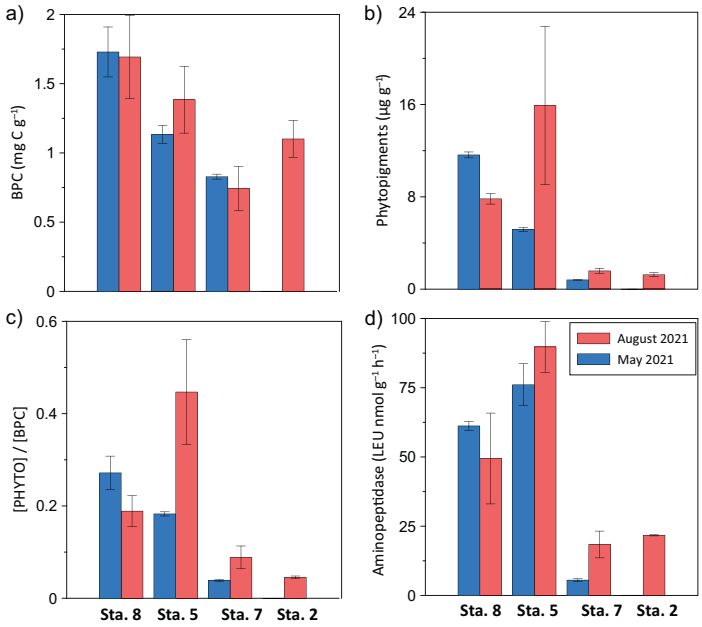

Fig. 3. Organic matter components and ratios at each station for both sampling times (August in red and May in blue) analyzed in the 0–0.5 cm sediment layer. Standard deviation was calculated from triplicates. No data were available for Sta. 2 in May 2021. (**a**) Biopolymeric carbon concentration (protein + carbohydrate + lipid concentration) (mg g^{-1}). (**b**) Phytopigment concentration (μg g^{-1}). (**c**) Phytopigment concentration over biopolymeric carbon concentration ratio. (**d**) Aminopeptidase (nmol g^{-1} h^{-1}).

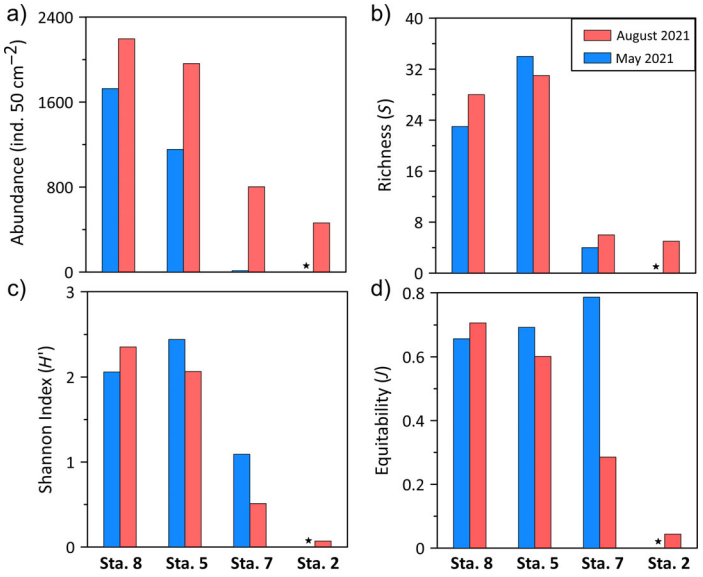

Fig. 4. Biodiversity metrics for the upper 5 cm of sediment during May and August 2021 sampling campaigns: (**a**) Normalized total foraminiferal abundances (ind. 50 cm^{-2}), (**b**) species richness (*S*), (**c**) Shannon index (*H'*), and (**d**) equitability index (*J*). Sta. 2 was barren in spring 2021 (star symbol).

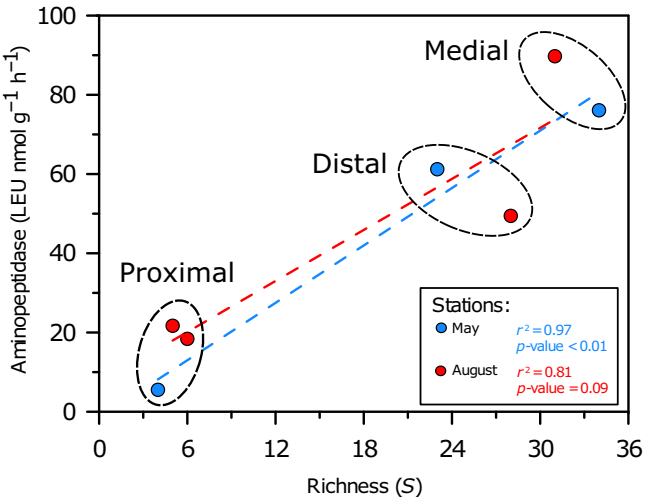

Fig. 5. Relationship between species richness (*S*) and associated aminopeptidase (LEU nmol g^{-1} h^{-1}) in the upper 0–0.5 cm of sediment at all stations, and both sampling times.

functioning) (Fig. 5) revealed a linear best fit in both seasons. Moreover, the relations found for the two seasons were observed by additional ANOVA analysis to be similar to each other ($p = 0.88$).

Species composition and vertical distribution. Figure 6 displays the vertical distribution of major species of living benthic foraminifera at the four stations along the fjord axis, in both spring and summer. Scanning electron micrographs of the main observed species are presented in Fig. S3.

Species diversities and densities can be observed according to species microhabitat (i.e., depth in sediment), which is why we have sampled and identified species in several intervals between 0 and 10 cm in the sediment.

Species assemblages and microhabitat distributions were noted at the proximal Stas. 2 and 7. In spring, no individuals were living in the sediment at the proximal Sta. 2. At the next proximal station, Sta. 7, only 25 ind. 50 cm^{-3} were found in the surface layers (0–1.5 cm), where the assemblage contained individuals of *Elphidium clavatum*, *Cassidulina reniforme*, *Triloculina oblonga*, and *Quinqueloculina seminula*. In summer, all living individuals at the proximal Stas. 2 and 7 were found in the upper 1–1.5 cm sediment, with a maximum at the topmost layer (0–0.5 cm). Living specimens in the surface layer (0–0.5 cm) reached densities of 800 and 1400 ind. 50 cm^{-3} at Stas. 2 and 7, respectively. Below 1.5 cm depth, no living specimen were recovered. At both stations faunas were dominated by *Capsammina bowmanni* (99% at Sta. 2 and 86% at Sta. 7).

At the medial Sta. 5, the surface layer (0–0.5 cm) contained 480 ind. 50 cm^{-3} of living foraminifera in spring. The surface assemblage was dominated by *Siphonaperta agglutinata*, *Reophax fusiformis*, *and Islandiella norcrossi/helenae*. The species *Nonionellina labradorica* showed a clear and gradual density increase down to 3 cm, followed by a clear decrease from

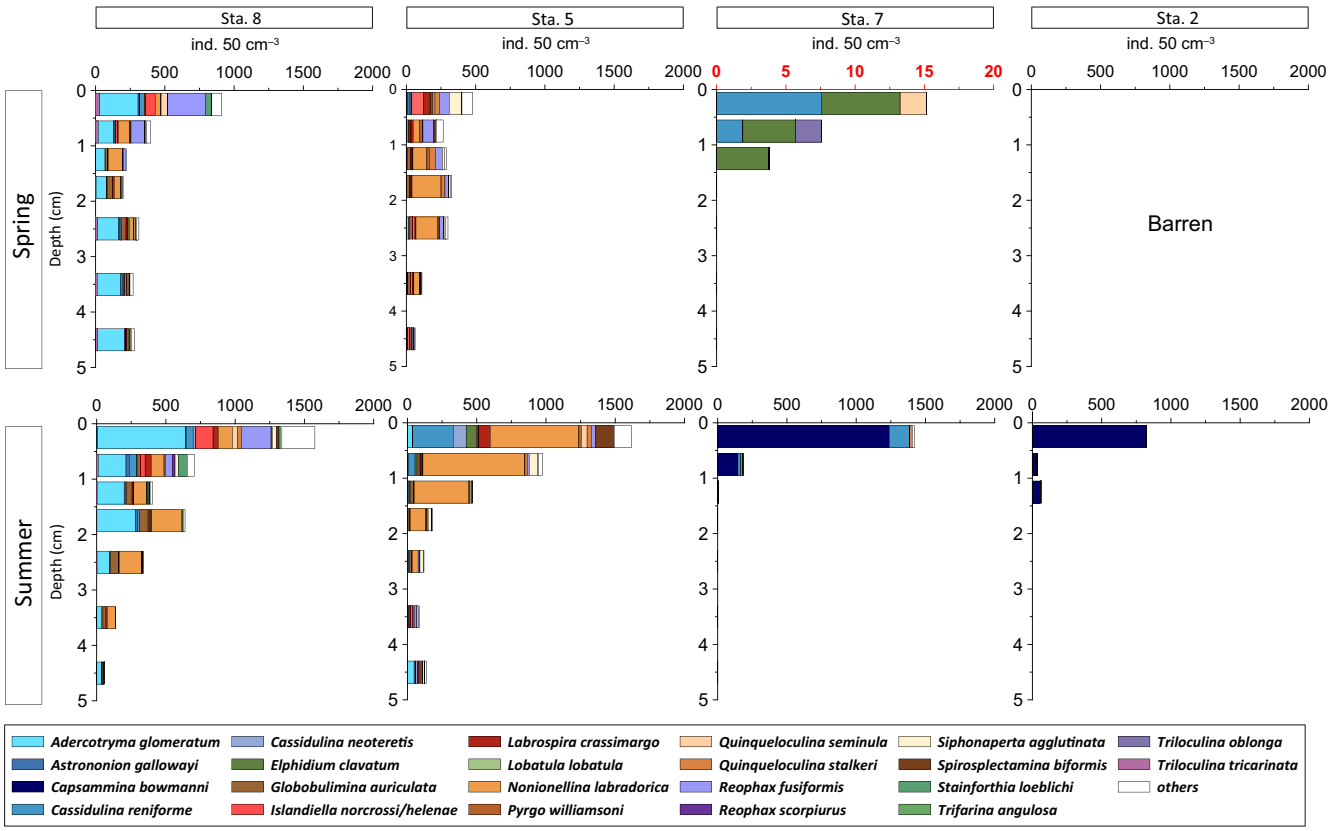

Fig. 6. Vertical distribution of the major foraminifera species (more than 5% in at least one sample) from the sediment surface down to 5 cm depth, at the four studied stations. The size fraction represented here is > 125 μm. The upper panel presents data from the spring campaign (May 2021) and the lower panel shows data from the summer campaign (August 2021). Note that the density scale for Sta. 7 in spring (in red) is 100 times lower than the others.

158 ind. 50 cm^{-3} at 3 cm depth to 42 ind. 50 cm^{-3} in the layer below. In summer, densities of living individuals decreased with depth, reaching a maximum of 1600 ind. 50 cm^{-3} at the surface and dropping to 130 ind. 50 cm^{-3} at 5 cm depth. The dominant species *N. labradorica* (50% of total fauna) showed a maximum density within the first centimeter of sediment and decreased until disappearing below 3 cm depth. Associated species *C. reniforme*, *Spiroplectamina biformis*, *Labrospira crassimargo*, and *E. clavatum* also decreased rapidly with depth. A small increase of *Adercotryma glomeratum* was observed between 4 and 5 cm, whereas it was present in low densities in the upper layers.

At the distal Sta. 8, in May 2021, foraminiferal density was maximum in the surface layer, with 910 ind. 50 cm^{-3}, and the dominant species were *A. glomeratum* (49% of fauna on the whole core) and *R. fusiformis* (11% of fauna on the whole core). Below, the abundance decreased, with *A. glomeratum* maintaining a slightly variable density of 200 ind. 50 cm^{-3} down to 5 cm depth. The density of all other species decreased with depth. Summer assemblages exhibited a bimodal vertical distribution of abundances. The first maximum of density was observed in the 0–0.5 cm layer, reaching 1600 ind. 50 cm^{-3}. The assemblage was mainly composed of *A. glomeratum* (38%), *N. labradorica* (21%), accompanied by minor species such as *I. norcrossi/helenae* and *R. fusiformis*. The second peak in abundance (700 ind. 50 cm^{-3}) was found between 1.5 and 2 cm depth, and contained mostly *A. glomeratum* and *N. labradorica* specimens.

Redundancy analysis. In addition to the foraminiferal vertical distribution, a redundancy analysis was performed to identify potential links between environmental factors and the spatial foraminiferal distribution along the fjord axis (Fig. 7). Five parameters were identified as non-colinear and significant predictors of variations in species abundances at each site for both seasons: mean turbidity values in the upper 20 m of the water column, water depth of the sampling site, concentration in phytopigments in the uppermost first centimeter of sediment, aminopeptidase values, salinity, and temperature of the bottom water (Fig. 7).

The RDA1 and RDA2 axes explain 84.1% of the total variance ($r^2 = 0.64$). The first axis shows a positive correlation with depth, phytopigments, aminopeptidase, and salinity, and a negative correlation with turbidity and temperature. This RDA1 axis also clearly separates the proximal Stas. 2 and 7 from the distal Sta. 8 and medial Sta. 5, in summer. The

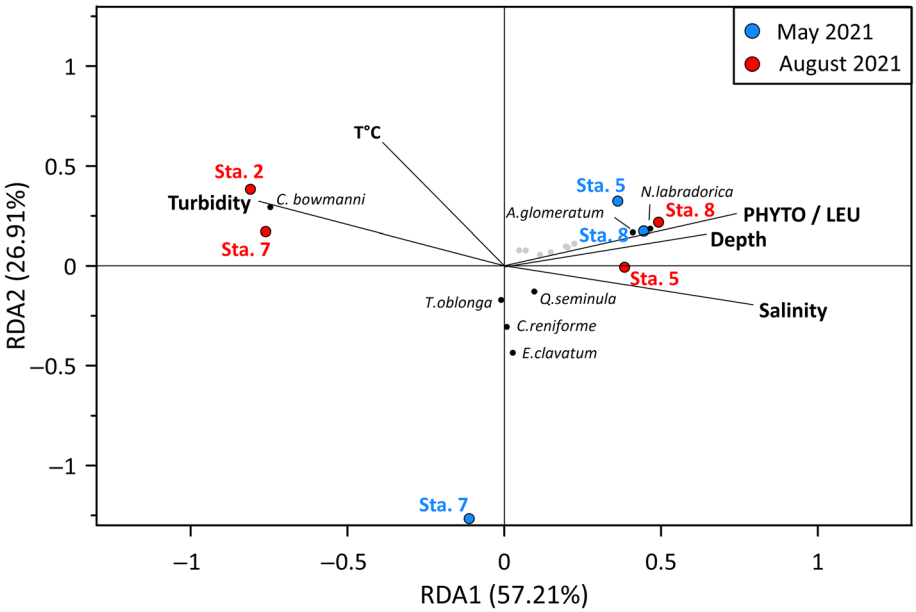

Fig. 7. Transformed-based redundancy analysis (tb-RDA) performed on the species abundances of living foraminifera within the 1st 0–5 cm of sediment at each sampling site both in May and August, considering the > 125 μm size fraction. Significative environmental parameters are displayed by the continuous black lines and their length correspond to the importance of the variable to explain the variance in the abundance matrix. The mean turbidity value was calculated from measurements taken in the upper 20 m of the water column, PHYTO is the sum of chlorophyll *a* and phaeopigment concentrations in the 1st 0–0.5 cm of sediment (μg g^{-1}), Depth is the sampling water depth (m), salinity, T°C are the bottom water values measured by CTD probes at each site and LEU is the leucine-aminopeptidase (nmol g^{-1} h^{-1}) in the 1st 0–0.5 cm of sediment. Data from Sta. 2 in May were not included in this analysis.

proximal stations are highly correlated with turbidity and slightly less with temperature, while the medial/distal stations are highly correlated with phytopigments, aminopeptidase, and depth. In August, the foraminiferal composition at Sta. 5 showed a combined effect of salinity, depth, and phytopigments concentration on its variance. The species with the highest correlation scores were *C. bowmanni* ($x = -0.6$; Stas. 2 and 7), *N. labradorica* and *A. glomeratum* ($x > 0.5$; Stas. 8 and 5).

Discussion

Seasonal environmental dynamics

The yearly water mass dynamic in Kongsfjorden, mainly described by Svendsen et al. (2002) and Cottier et al. (2005), were well represented by our CTD data that showed a strong contrast between the homogeneous water column during spring (with winter cooled waters at proximal Stas. 2 and 7 and local waters at Stas. 5 and 8) and the highly stratified one in summer 2021 (Fig. 2).

The temperature, salinity, Chl *a* concentration, and turbidity regimes largely changed between the two seasons, as a result of the entries of AW during summer and the reactivation of the melting phase of the Kronebreen glacier generating the freshwater layer (surface water) above the Atlantic current (transformed AW) (Fig. 2).

In Svalbard fjords, the variations in water turbidity and phytoplanktonic growth, highly depending on seasonal dynamic (Piquet et al. 2014; Calleja et al. 2017) have a strong influence on benthic environments, in terms of sedimentary stability (e.g., Mestdagh et al. 2018; Guilhermic et al. 2023) and organic supply (e.g., Bourgeois et al. 2016).

As observed and described by D'Angelo et al. (2018) and Meslard et al. (2018), the surface turbidity in Kongsfjorden originates from glacier melting and subglacial runoff. This freshwater flow concentrates detrital particles eroded the catchment bedrock and delivers them at the base of the glacier to the fjord (Meslard et al. 2018). Density differences generate an upwelling and creates a surface current spreading in the fjord. The surface of spreading can change at high frequency due to tide, wind regimes, and water flux from the glacier (Trusel et al. 2010). According to D'Angelo et al. (2018), sediment inputs mostly occur between July and September (38–71% of the annual detrital mass flux between 2010 and 2016). This is consistent with our CTD observations, which showed 50 times higher turbidity in August compared to May 2021 at the closest glacier stations (Fig. 2). Lydersen et al. (2014) reported decreasing sedimentation rates with increasing distance from Kronebreen front, as calculated from a model based on data from July 2003. Sedimentation rates can reach 800 g m^{-2} d^{-1} near the glacier front (Lydersen et al. 2014) and at least 60–90 mm yr^{-1} in most glacier proximal areas due to Kronebreen subglacial runoff (Trusel et al. 2010). Sedimentation rates beyond the Lovénøyane sill are two times lower. Based on the same model, the mean sedimentation rate can be estimated below 25 g m^{-2} d^{-1} at the

location of our Stas. 8 and 5. According to these estimations, and following our CTD data, it can be inferred that the sediment supply to the bottom and the resulting physical instability of the benthic habitats decrease as the distance from Kronebreen front increases.

During spring, in parallel of nearly zero turbidity, our CTD data showed a limited phytoplanktonic growth whereas a strong antagonistic gradient between these two parameters was found in the surface water of the fjord in summer. At this season, the increase of turbidity deriving from glacier melt waters, limited the phytoplanktonic growth at the glacier-proximal stations (Fig. 2). Away from the glacier, as far as turbidity abruptly decreased on the fringe of the turbid plume, Chl *a* concentrations increase through two processes (Lydersen et al. 2014): (1) enhanced nutrient transport toward the surface by subglacial upwelling and (2) higher light penetration that promotes photosynthesis. This is consistent with Calleja et al. (2017) and Piquet et al. (2014) who described phytoplanktonic bloom episodes occurring far from the glacier fronts during summer.

On the other hand, the low and spatially relatively homogenous Chl *a* concentrations we measured in spring did not clearly support the occurrence of the expected phytoplanktonic spring bloom at the sampling time.

Despite this high contrast among seasons, however, the organic matter parameters we measured in the sediment (Fig. 3) showed that the spatial gradient along the transect was much steeper than seasonal differences within a same station. Indeed, except for phytopigments, which were particularly higher during summer at Sta. 5 (i.e., reflecting the high Chl *a* concentrations observed at the fringes of the turbid plume), an increasing gradient in organic matter quality (BPC) and freshness (phytopigments) was visible along the transect, from the proximal to the distal zone, at both seasons (Fig. 3). In this geographical area, the organic matter deposited on the seafloor is supposed to mostly originate from the biological production in the water column (i.e., vertical fluxes) as reported by Bourgeois et al. (2016). Therefore, the zones of higher primary production should coincide with the ones of higher accumulation at the seabed. If this corresponded to the summer conditions (Fig. 2), this was not the case for spring conditions, where there were no differences among the stations in terms of Chl *a* concentrations. While, at the proximal stations, the dilution and turbidity due to sediment supply limited the accumulation of organic matter (Fig. 3), at the medial to distal stations, the conservation of organic matter exported during summer could be a possible explanation of the relative homogeneity of the OM parameters among seasons. Indeed, we suggest that the food bank theory postulated by Mincks et al. (2005) in Antarctica can be extended to this region as well. This theory postulates that, at low Antarctica temperatures, the yearly availability of labile organic matter in the sediment stays relatively stable thanks to low bacterial remineralization, resulting in a long-term sediment food bank for detritivores. This is particularly the case of Sta. 8, where the differences in BPC, Phyto/BPC, and aminopeptidase were not significant between the sampled seasons (Fig. 3). Consistently with Mincks et al. (2005), at this station, the primary production in summer (represented by higher phytopigments; Fig. 3b) did not affect the microbial activity and ecosystem functioning (represented by aminopeptidase), indicating that bacteria did not respond to fresh phytodetritus. Differently, the strongest extracellular degradation rates (i.e., leucine aminopeptidase) were recorded on the fringe of the turbid plume during summer, where the turbidity stress decreases and nutrient export from melting water supports higher primary production. At this station, therefore, the ecological functioning was higher and the benthic consumption of fresh organic matter potentially more efficient than at distal Sta. 8 (Pusceddu et al. 2014).

Benthic community responses to seasonal and spatial gradients

Spatial distribution of foraminiferal assemblages was investigated in relation with environmental gradients and their seasonal variations. Previous studies conducted in Kongsfjorden highlighted a high spatial variability during summer in terms of biodiversity and abundance of benthic foraminifera (e.g., Jernas et al. 2018; Fossile et al. 2022). This variability was mainly attributed to bottom water masses (e.g., Atlantic vs. Arctic water bodies, as noted by Jernas et al. 2018) and physical disturbance induced by glacier fronts in the inner basin (Fossile et al. 2022) during the melting season.

Our research highlights the role of seasonal contrast in environmental drivers of this spatial gradient. In addition to the parameters already analyzed in the previous studies, we focused on the availability of organic matter instead of total organic C, as benthic foraminifera are expected to respond to the concentration and quality of the available fraction of organic carbon (e.g., Nardelli et al. 2010). The data we collected at the two seasons showed a gradient of decreasing abundances and diversity of benthic foraminifera, moving toward the glacier front (Fig. 4). Fossile et al. (2022) reported the same gradient, which they attributed to environmental stress induced by glacier melting during summer. Similarly to Fossile et al. (2022), we found in summer a few species only at the surface of the sediment at the glacier proximal Stas. 2 and 7 (*C. bowmanni* and *C. reniforme*). RDA showed a high correlation between the presence of these major species, high turbidity and low phytopigment contents in summer (Fig. 7). The presence of the agglutinated species *C. bowmanni* in the uppermost centimeter of the sediment was already reported in other Arctic fjords by Gooday et al. (2010). Following these authors, this species displays opportunistic or pioneer behavior in stressful environments. This is in line with the high abundances and the strong dominance of *C. bowmanni* in the assemblages observed in the first centimeter at Stas. 2 and 7 in

summer, when labile organic matter is scarce. Also, the limitation of the nearly monospecific faunas in the uppermost layers of the sediment at the proximal stations further indicates that habitat restrictions were possibly related both to physical disturbance due to high sedimentation rate and food limitations (*see* Trox model, Jorissen 1999). In addition, the fjord receives, during summer, a high supply of micas from bedrocks of Kronebreen ice shed (Dallmann 2015). This could represent a further advantage for the summer development of *C. bowmanni*, as this species exclusively builds its agglutinated test with mica minerals (Gooday et al. 2010). During spring, the lower stress conditions induced by reduced sedimentation did not benefit other species. The two stations were nearly or completely barren, probably due to the very low organic matter content (as also confirmed by the almost null bacterial activity, i.e., aminopeptidase, Fig. 3). The few individuals (13; Fig. 6) found in Sta. 7 belonged to the species *C. reniforme* and *E. clavatum*, that are known to be opportunists in the proximity of glacier fronts (Hald and Korsun 1997; Fossile et al. 2020, 2022).

Further from the Kronebreen glacier front and beyond the Lovenøyane sill, abundances and biodiversity throughout the cores at medial Sta. 5 were much higher compared to the glacier proximal stations. This is consistent with the findings of Fossile et al. (2022), which suggested that the overall increase in diversity and abundance of living benthic foraminifera is associated with the reduction of the stress induced by glacier proximity, represented by detrital sedimentation and limited primary production. However, we observed important differences between the two sampled seasons at this station. Abundances were twice as high in summer compared to spring, which further suggests that food limitation (Fig. 3) was the primary cause of low abundances in spring. Considering the total fauna, *N. labradorica* was the dominant species in both spring (35%) and summer (50%), accompanied by several minor species (*L. crassimargo*, *R. fusiformis*, and *S. agglutinata*). *Nonionellina labradorica* was previously described as feeding on fresh phytodetritus and associated with OM-enriched AW intrusions during summer (Hald and Korsun 1997; Fossile et al. 2022). This species is predominantly found in the upper centimeter of sediment, as observed in these previous studies and in our summer samples. Organic matter data obtained at the same period showed that in summer, Sta. 5 had the highest Chl *a* concentration, [Phyto]/[BPC] values and aminopeptidase rates compared to the other stations (Fig. 3c). This indicates a higher export of fresh phytodetritus to the seabed and increased extracellular bacterial activity in the sediment. Moreover, the maximum abundance of *N. labradorica* in the uppermost layers of sediment further suggests the vertical export of OM at this station during summer (Fig. 3). Despite the presence of completely different water masses recorded at the seabed and a trophic regime that was largely poorer than in summertime, *N. labradorica* was still largely present in spring. This suggests, that its presence is not systematically related to the presence of AW, as previously hypothesized by Hald and Korsun (1997) and Kucharska et al. (2019), and that this species has the capacity to adapt to very changing environmental conditions. One possible strategy could be a change in preferential microhabitat. Indeed, in spring, the species was poorly represented in surface layers and showed its maximum density at 1.5–2 cm depth in sediment. The preference for infaunal microhabitats in spring suggests that this species may be able to use alternative food sources when fresh phytodetritus is not available. This includes older and buried organic matter, as evidenced by lower values of the [PRT]/[CHO] ratio (Fig. 3), in accord with the "food bank" theory (Mincks et al. 2005). The ability to switch between shallow and intermediate infaunal preferential microhabitats could also be due to the possibility for this species to use denitrification as an alternative metabolism, as suggested by Woehle et al. (2022). Other hypotheses can be proposed to explain the different vertical distribution of *N. labradorica* and associated species between spring and summer. These hypotheses may include different conditions in physical stability, driven, for example, by higher bioturbation or the possibility that the surface peak of the species in summer is due to a recent reproductive event, which generally occurs near the sediment surface. This last hypothesis does not seem to be supported by the sizes of the picked specimens (between 125 and 63 μm fraction checked for confirmation), which are not noticeably different from those of spring and do not show the presence of juveniles. A significant change in the seasonal influence of bioturbation on the stability of macro- and meiofaunal communities (except foraminifera) in the fjord was not observed in previous studies in shallow or deep benthic environments (Kędra et al. 2011; Włodarska-Kowalczuk et al. 2016; Hop and Wiencke 2019), as no seasonal changes in standing stocks and diversity were observed.

At Sta. 8, the most distal station from the Kronebreen glacier front, the species composition of foraminiferal assemblages was highly correlated with phytopigment content and water depth, at both seasons (Fig. 7). Despite relatively lower abundances and biodiversity in spring compared to summer, the major species of the total fauna present throughout the sediment cores at the two seasons were the same, *Adercotryma glomeratum* and *Nonionellina labradorica*. The first species was always more abundant, particularly during summer. At this season, *A. glomeratum* was previously observed and linked to AW influence (Tesi et al. 2021). This species was supposed to benefit from high quantity of low quality organic matter (e.g., Hald and Korsun 1997; Jernas et al. 2018). Although TAW was only present in summer in our dataset, the direct link with AW does not seem to be confirmed, as *A. glomeratum* was recorded in both seasons. On the opposite, the ability to feed on low quality organic matter appears to be an advantage in competition with the second major species, *N. labradorica*, as previously suggested by Fossile et al. (2022), and totally in agreement with our hypothesis of the presence of a "food bank" for detritivores in this area of the fjord. Indeed, the Phyto/BPC ratios at this station are similar to each other and

lower than at Sta. 5 in summer and near the value found in spring (Fig. 3c). In contrast to the former, *A. glomeratum* was dominant in the superficial layers at Sta. 8, while *N. labradorica* was only present in more infaunal microhabitats (0.5–3 cm depth). This vertical distribution could be attributed to a weaker competitive ability of *N. labradorica* against *A. glomeratum* under low quality food regimes. This competition was even more pronounced in summer when the Phyto/BPC ratios at Sta. 8 were noticeably lower than those in spring.

Implications on ecosystem functioning

In soft bottom environments, the spatial succession of communities from highly disturbed to physically undisturbed habitats was already observed for both meiofauna and macrofauna (Conlan and Kvitek 2005; Pasotti et al. 2015). In disturbed conditions, pioneer taxa can recolonize newly deposited sediment when environmental conditions become favorable. This recolonization leads to a gradual increase in faunal abundances after disturbance and associated extermination, without exceeding the abundances observed in unscoured areas. This seems to be the case for of *C. bowmanni* in our glacier proximal stations.

Reduced turbidity and sedimentation were reported to result in a complexity increase of community structure and functional diversity for macrofauna (Elverhøi et al. 1983; Wlodarska-Kowalczuk and Pearson 2004; Kędra et al. 2010) and foraminifera (Fossile et al. 2022). The increasing sediment stability down-fjord has a positive effect on the colonization of the benthic environment (Hop and Wiencke 2019). At medial Sta. 5, beyond the inner sill, the highest values of species richness and aminopeptidase (extracellular OM degradation) were observed, suggesting higher ecosystem functioning in the area (Figs. 3 and 4). These observations could result from a shallower depth at Sta. 5 compared to the most glacier distal Sta. 8 and a more efficient export of fresh organic matter to the seabed and/or the result of intermediate disturbance conditions (Connell 1978), as Sta. 5 is located in the middle zone of the turbidity gradient. In accordance with the theory of Connell (1978), the intermediate disturbance is the key for higher diversity as the middle point between rough conditions which tends to limit the sensitive species and stable good environmental conditions where diversity is mainly driven by interspecies competition. In these habitats, species would tend to be less generalist and less redundant to maximize resource exploitation, which in turns represents a higher vulnerability toward changes. This kind of habitats should therefore be particularly observed as they constitute early witnesses in front of future environmental changes.

Our data on both medial and distal areas globally suggest that the seasonal discharges of sediment during the ice-melting season in this inner part of the fjord are the driver of the observed environmental and faunal gradients and have cascade effects on primary production, organic degradation and ecosystem functioning in the distal area. The effects of spatial and temporal amplitude of turbidity and physical instability on benthic communities in this area may be influenced by interannual variations of Kronebreen subglacial discharge.

In the near future, the seasonality of hydrography, primary production, and glacier melting yearly dynamics is expected to become less pronounced (Hop and Wiencke 2019; Payne and Roesler 2019) and this could lead to drastic changes in the weak equilibrium we described. On a short time scale (10 yr; IPCC 2022), the inflow of AW could occur earlier in the year and extend throughout the warm season in the fjord. This could lead to increased melting of tidewater glaciers, water stratification, limited spring blooms, and increased turbidity due to higher sediment discharges (Piquet et al. 2014; Payne and Roesler 2019). This would push down-fjord the conditions observed today in the proximal stations, resulting in a decrease in ecological functioning in the innermost basin. Additionally, the imminent surge of the Kongsvegen glacier, which shares its front with the Kronebreen was hypothesized by Bouchayer et al. (2023), who observed an acceleration of the glacier downstream velocity from 6 m yr^{-1} in 2014 to almost 40 m yr^{-1} in 2022. A surge event would move the glacier front down-fjord on a kilometric scale within several weeks/months, with a further potential shift of the unstable sediment area down-fjord.

In a longer-term scenario, the Kronebreen is expected to retreat on land and the consequent sediment discharge would drastically decrease. It would lead to reduced turbidity and nutrient inputs into the fjord and result in larger, but possibly poorer, stable areas at the fjord head. All these scenarios highlight the urgent need for monitoring programs to better constrain the consequences of ongoing climate changes on the ecological functioning on these vulnerable ecosystems.

Conclusions

This study highlights the effects of glacier melting-induced environmental gradients on the seasonal distribution of benthic foraminifera. The three previously determined summer biozones were proven to be recognizable also during spring but seasonal changes were observed. Highly contrasted water mass distribution, turbidity, primary production, and resulting sedimentary organic carbon and sediment instability were proven to be the main drivers of foraminiferal patterns between the two considered seasons. The most glacier proximal stations showed low diversity and pioneer species dominance in summer, in response to low OM export and high sedimentation from glacier melting. In spring they are barren or poor in individuals due to low OM contents (no or low food bank effect). As the influence of the surface turbid plume decreases with distance from the Kronebreen glacier front, the benthic environmental conditions become more favorable for foraminiferal community development during summer in the medial and distal areas. Organic matter availability and sediment stability enhance equilibrated and rich assemblages.

During spring the assemblages are similar in species composition but less abundant, as a result of lower OM export from the water column. The more infaunal vertical distribution of the main species suggests that the burial of undegraded organic matter from summer exports can sustain strong ecosystem functioning during the whole year, in accord with the "food bank" theory.

In view of increasing glacier melting in the next future, the regional biodiversity of the fjord and the efficiency of the food bank are expected to decrease, because of the expansion of the areas submitted to sediment discharges. The consequences on benthic ecosystem functioning will be observable through the study of foraminiferal assemblages.

Data availability statement

Raw data presented in this manuscript will be available in an online repository upon the publication of the study.

References

Blott, S. J., and K. Pye. 2001. GRADISTAT: A grain size distribution and statistics package for the analysis of unconsolidated sediments. Earth Surf. Process. Landf. **26**: 1237–1248. doi:10.1002/esp.261

Bouchayer, C., U. Nanni, P.-M. Lefeuvre, J. Hulth, L. Steffensen Schmidt, J. Kohler, F. Renard, and T. V. Schuler. 2023. Multi-scale variations of hydro-mechanical conditions at the base of the surge-type glacier Kongsvegen, Svalbard. EGUsphere. **18**: 2939–2968. doi:10.5194/egusphere-2023-618

Bouchet, V. M. P., R. J. Telford, B. Rygg, E. Oug, and E. Alve. 2018. Can benthic foraminifera serve as proxies for changes in benthic macrofaunal community structure? Implications for the definition of reference conditions. Mar. Environ. Res. **137**: 24–36. doi:10.1016/j.marenvres.2018.02.023

Bourgeois, S., P. Kerhervé, M. L. Calleja, G. Many, and N. Morata. 2016. Glacier inputs influence organic matter composition and prokaryotic distribution in a high Arctic fjord (Kongsfjorden, Svalbard). J. Mar. Syst. **16**:112–127.

Calleja, M. L., P. Kerhervé, S. Bourgeois, M. Kędra, A. Leynaert, E. Devred, M. Babin, and N. Morata. 2017. Effects of increase glacier discharge on phytoplankton bloom dynamics and pelagic geochemistry in a high Arctic fjord. Prog. Oceanogr. **159**: 195–210. doi:10.1016/j.pocean.2017.07.005

Conlan, K., and R. Kvitek. 2005. Recolonization of soft-sediment ice scours on an exposed Arctic coast. Mar. Ecol. Prog. Ser. **286**: 21–42. doi:10.3354/meps286021

Connell, J. H. 1978. Diversity in tropical rain forests and coral reefs: High diversity of trees and corals is maintained only in a nonequilibrium state. Science **199**: 1302–1310. doi:10.1126/science.199.4335.1302

Cottier, F., V. Tverberg, M. Inall, H. Svendsen, F. Nilsen, and C. Griffiths. 2005. Water mass modification in an Arctic fjord through cross-shelf exchange: The seasonal hydrography of Kongsfjorden, Svalbard. J. Geophys. Res. **110**: C12005. doi:10.1029/2004JC002757

D'Angelo, A., F. Giglio, S. Miserocchi, A. Sanchez-Vidal, S. Aliani, T. Tesi, A. Viola, M. Mazzola, and L. Langone. 2018. Multi-year particle fluxes in Kongsfjorden, Svalbard. Biogeosciences **15**: 5343–5363. doi:10.5194/bg-15-5343-2018

Dallmann, W. K. 2015. Geoscience atlas of Svalbard. Norsk Polarinstitutt.

Danovaro, R. [ed.]. 2009. Methods for the study of deep-sea sediments, their functioning and biodiversity. CRC Press. doi:10.1201/9781439811382

Divya, D. T., and K. P. Krishnan. 2017. Recent variability in the Atlantic water intrusion and water masses in Kongsfjorden, an Arctic fjord. Pol. Sci. **11**: 30–41. doi:10.1016/j.polar.2016.11.004

Elverhøi, A., Ø. Lønne, and R. Seland. 1983. Glaciomarine sedimentation in a modern fjord environment, Spitsbergen. Polar Res. **1**: 127–149. doi:10.3402/polar.v1i2.6978

Fabiano, M., R. Danovaro, and S. Fraschetti. 1995. A three-year time series of elemental and biochemical composition of organic matter in subtidal sandy sediments of the Ligurian Sea (northwestern Mediterranean). Cont. Shelf Res. **15**: 1453–1469. doi:10.1016/0278-4343(94)00088-5

Fossile, E., and others. 2020. Benthic foraminifera as tracers of brine production in the Storfjorden "sea ice factory". Biogeosciences **17**: 1933–1953. doi:10.5194/bg-17-1933-2020

Fossile, E., M. P. Nardelli, H. Howa, A. Baltzer, Y. Poprawski, I. Baneschi, M. Doveri, and M. Mojtahid. 2022. Influence of modern environmental gradients on foraminiferal faunas in the inner Kongsfjorden (Svalbard). Mar. Micropaleontol. **173**: 102117. doi:10.1016/j.marmicro.2022.102117

Gooday, A. J., B. Lecroq, and R. B. Pearce. 2010. The "mica sandwich"; a remarkable new genus of Foraminifera (Protista, Rhizaria) from the Nazaré Canyon (Portuguese margin, NE Atlantic). Micropaleontology **56**: 345–357.

Guilhermic, C., M. P. Nardelli, A. Mouret, D. Le Moigne, and H. Howa. 2023. Short-term response of benthic foraminifera to fine sediment depositional events simulated in microcosm. Biogeosciences **20**: 1–46. doi:10.5194/bg-2023-31

Halbach, L., and others. 2019. Tidewater glaciers and bedrock characteristics control the phytoplankton growth environment in a fjord in the Arctic. Front. Mar. Sci. **6**: 254. doi:10.3389/fmars.2019.00254

Hald, M., and S. Korsun. 1997. Distribution of modern benthic foraminifera from fjords of Svalbard, European Arctic. J. Foraminiferal Res. **27**: 101–122. doi:10.2113/gsjfr.27.2.101

Hegseth, E. N., and others. 2019. Phytoplankton seasonal dynamics in Kongsfjorden, Svalbard and the adjacent shelf, p. 173–227. *In* H. Hop and C. Wiencke [eds.], The ecosystem of Kongsfjorden, Svalbard, v. **2**. Springer International Publishing. doi:10.1007/978-3-319-46425-1_6

Hop, H., and C. Wiencke [eds.]. 2019. The ecosystem of Kongsfjorden, Svalbard. Springer International Publishing. doi:10.1007/978-3-319-46425-1

Hoppe, C. J. M. 2022. Always ready? Primary production of Arctic phytoplankton at the end of the polar night. Limnol. Oceanogr. Lett. **7**: 167–174. doi:10.1002/lol2.10222

Howe, J. A., S. G. Moreton, C. Morri, and P. Morris. 2003. Multibeam bathymetry and the depositional environments of Kongsfjorden and Krossfjorden, western Spitsbergen, Svalbard. Polar Res. **22**: 301–316. doi:10.1111/j.1751-8369.2003.tb00114.x

Howe, J. A., W. E. N. Austin, M. Forwick, M. Paetzel, R. Harland, and A. G. Cage. 2010. Fjord systems and archives: A review. Geol. Soc. Spec. Pub. **344**: 5–15. doi:10.1144/SP344.2

Husum, K., and others. 2019. The marine sedimentary environments of Kongsfjorden, Svalbard: An archive of polar environmental change. Polar Res. **38**. doi:10.33265/polar.v38.3380

Intergovernmental Panel on Climate Change (IPCC). 2022. The ocean and cryosphere in a changing climate: Special report of the intergovernmental panel on climate change, 1st ed. Cambridge Univ. Press. doi:10.1017/9781009157964

IPCC. 2023. Summary for policymakers, p. 1–34. *In* H. Lee and J. Romero [eds.], Climate change 2023: Synthesis report. Contribution of working groups I, II and III to the sixth assessment report of the intergovernmental panel on climate change. IPCC. doi:10.59327/IPCC/AR6-9789291691647.001

Iona, A., A. Theodorou, S. Watelet, C. Troupin, and J.-M. Beckers. 2018. Mediterranean sea hydrographic atlas: Towards optimal data analysis by including time-dependent statistical parameters. Earth Syst. Sci. Data. **10**: 1281–1300. doi:10.5194/essd-2018-9

Jernas, P., D. Klitgaard-Kristensen, K. Husum, N. Koç, V. Tverberg, P. Loubere, M. Prins, N. Dijkstra, and M. Gluchowska. 2018. Annual changes in Arctic fjord environment and modern benthic foraminiferal fauna: Evidence from Kongsfjorden, Svalbard. Global Planet. Change **163**: 119–140. doi:10.1016/j.gloplacha.2017.11.013

Jima, M., P. R. Jayachandran, and S. Bijoy Nandan. 2022. Modern benthic foraminiferal diversity along the fjords of Svalbard archipelago: Diversity evaluation. Thalassas **38**: 647–664. doi:10.1007/s41208-021-00356-7

Jorissen, F. J. 1999. Benthic foraminiferal microhabitats below the sediment-water interface, p. 161–179. *In* Modern Foraminifera. Springer Netherlands. doi:10.1007/0-306-48104-9_10

Jorissen, F. J., H. C. de Stigter, and J. G. V. Widmark. 1995. A conceptual model explaining benthic foraminiferal microhabitats. Mar. Micropaleontol. **26**: 3–15. doi:10.1016/0377-8398(95)00047-X

Jorissen, F. J., M. P. A. Fouet, D. Singer, and H. Howa. 2022. The marine influence index (MII): A tool to assess estuarine intertidal mudflat environments for the purpose of foraminiferal biomonitoring. Water **14**: 676. doi:10.3390/w14040676

Kędra, M., M. Włodarska-Kowalczuk, and J. M. Węsławski. 2010. Decadal change in macrobenthic soft-bottom community structure in a high Arctic fjord (Kongsfjorden, Svalbard). Polar Biol. **33**: 1–11. doi:10.1007/s00300-009-0679-1

Kędra, M., J. Legeżyńska, and W. Walkusz. 2011. Shallow winter and summer macrofauna in a high Arctic fjord (79°N, Spitsbergen). Mar. Biodiv. **41**: 425–439. doi:10.1007/s12526-010-0066-8

Kucharska, M., A. Kujawa, J. Pawłowska, M. Łącka, N. Szymańska, O. J. Lønne, and M. Zajączkowski. 2019. Seasonal changes in foraminiferal assemblages along environmental gradients in Adventfjorden (West Spitsbergen). Polar Biol. **42**: 569–580. doi:10.1007/s00300-018-02453-5

Lind, S., R. B. Ingvaldsen, and T. Furevik. 2018. Arctic warming hotspot in the northern Barents Sea linked to declining sea-ice import. Nat. Clim. Change **8**: 634–639. doi:10.1038/s41558-018-0205-y

Lorenzen, C., and J. Jeffrey. 1980. Determination of chlorophyll in seawater. UNESCO Tech. Pap. Mar. Sci. **35**: 1–20.

Lydersen, C., and others. 2014. The importance of tidewater glaciers for marine mammals and seabirds in Svalbard, Norway. J. Mar. Syst. **129**: 452–471. doi:10.1016/j.jmarsys.2013.09.006

Meslard, F., F. Bourrin, G. Many, and P. Kerhervé. 2018. Suspended particle dynamics and fluxes in an Arctic fjord (Kongsfjorden, Svalbard). Estuar. Coast. Shelf Sci. **204**: 212–224. doi:10.1016/j.ecss.2018.02.020

Mestdagh, S., L. Bagaço, U. Braeckman, T. Ysebaert, B. De Smet, T. Moens, and C. Van Colen. 2018. Functional trait responses to sediment deposition reduce macrofauna-mediated ecosystem functioning in an estuarine mudflat. Biogeosciences **15**: 2587–2599. doi:10.5194/bg-15-2587-2018

Mincks, S., C. Smith, and D. DeMaster. 2005. Persistence of labile organic matter and microbial biomass in Antarctic shelf sediments: Evidence of a sediment food bank. Mar. Ecol. Prog. Ser. **300**: 3–19. doi:10.3354/meps300003

Nardelli, M. P., F. J. Jorissen, A. Pusceddu, C. Morigi, A. Dell'Anno, R. Danovaro, H. C. De Stigter, and A. Negri. 2010. Living benthic foraminiferal assemblages along a latitudinal transect at 1000m depth off the Portuguese margin. Micropaleontology **56**: 323–344.

Notz, D., and J. Stroeve. 2016. Observed Arctic sea-ice loss directly follows anthropogenic CO_2 emission. Science **354**: 747–750. doi:10.1126/science.aag2345

Oksanen, J., F. Guillaume Blanchet, M. Friendly, R. Kindt, P. Legendre, D. McGlinn, P. R. Minchin, R. B. O'Hara, G. L. Simpson, S. Peter, M. Henry, H. Stevens, E. Szoecs, H. Wagner, 2015. vegan: community ecology package. In: R package version 2.5-6. https://CRAN.R-project.org/package=vegan.

Pasotti, F., E. Manini, D. Giovannelli, A.-C. Wölfl, D. Monien, E. Verleyen, U. Braeckman, D. Abele, and A. Vanreusel. 2015. Antarctic shallow water benthos in an area of recent rapid glacier retreat. Mar. Ecol. **36**: 716–733. doi:10.1111/maec.12179

Payne, C. M., and C. S. Roesler. 2019. Characterizing the influence of Atlantic water intrusion on water mass formation and phytoplankton distribution in Kongsfjorden, Svalbard. Cont. Shelf Res. **191**: 104005. doi:10.1016/j.csr.2019.104005

Perovich, D. K., and J. A. Richter-Menge. 2009. Loss of sea ice in the Arctic. Ann. Rev. Mar. Sci. **1**: 417–441. doi:10.1146/annurev.marine.010908.163805

Piquet, A. M.-T., W. H. van de Poll, R. J. W. Visser, C. Wiencke, H. Bolhuis, and A. G. J. Buma. 2014. Springtime phytoplankton dynamics in Arctic Krossfjorden and Kongsfjorden (Spitsbergen) as a function of glacier proximity. Biogeosciences **11**: 2263–2279. doi:10.5194/bg-11-2263-2014

Pusceddu, A., and others. 2010. Organic matter in sediments of canyons and open slopes of the Portuguese, Catalan, Southern Adriatic and Cretan Sea margins. Deep-Sea Res. I Oceanogr. Res. Pap. **57**: 441–457. doi:10.1016/j.dsr.2009.11.008

Pusceddu, A., S. Bianchelli, J. Martín, P. Puig, A. Palanques, P. Masqué, and R. Danovaro. 2014. Chronic and intensive bottom trawling impairs deep-sea biodiversity and ecosystem functioning. Proc. Natl. Acad. Sci. U. S. A. **111**: 8861–8866. doi:10.1073/pnas.1405454111

Richirt, J., B. Riedel, A. Mouret, M. Schweizer, D. Langlet, D. Seitaj, F. J. R. Meysman, C. P. Slomp, and F. J. Jorissen. 2020. Foraminiferal community response to seasonal anoxia in Lake Grevelingen (the Netherlands). Biogeosciences **17**: 1415–1435. doi:10.5194/bg-17-1415-2020

Richter, A., A. Groh, and R. Dietrich. 2012. Geodetic observation of sea-level change and crustal deformation in the Baltic Sea region. Phys. Chem. Earth A/B/C **53–54**: 43–53. doi:10.1016/j.pce.2011.04.011

Schlitzer, Reiner, Ocean data view, 2023. https://epic.awi.de/id/eprint/56921/

Strzelewicz, A., A. Przyborska, and W. Walczowski. 2022. Increased presence of Atlantic water on the shelf south-west of Spitsbergen with implications for the Arctic fjord Hornsund. Prog. Oceanogr. **200**: 102714. doi:10.1016/j.pocean.2021.102714

Svendsen, H., and others. 2002. The physical environment of Kongsfjorden–Krossfjorden, an Arctic fjord system in Svalbard. Polar Res. **21**: 133–166. doi:10.3402/polar.v21i1.6479

Tesi, T., and others. 2021. Rapid Atlantification along the Fram strait at the beginning of the 20th century. Sci. Adv. **7**: eabj2946. doi:10.1126/sciadv.abj2946

Trusel, L. D., R. D. Powell, R. M. Cumpston, and J. Brigham-Grette. 2010. Modern glacimarine processes and potential future behaviour of Kronebreen and Kongsvegen polythermal tidewater glaciers, Kongsfjorden, Svalbard. Geol. Soc. Spec. Pub. **344**: 89–102. doi:10.1144/SP344.9

Tverberg, V., R. Skogseth, F. Cottier, A. Sundfjord, W. Walczowski, M. E. Inall, E. Falck, O. Pavlova, and F. Nilsen. 2019. The Kongsfjorden transect: Seasonal and inter-annual variability in hydrography, p. 49–104. *In* H. Hop and C. Wiencke [eds.], The ecosystem of Kongsfjorden, Svalbard, v. **2**. Springer International Publishing. doi:10.1007/978-3-319-46425-1_3

van De Poll, W. H., D. S. Maat, P. Fischer, P. D. Rozema, O. B. Daly, S. Koppelle, R. J. W. Visser, and A. G. J. Buma. 2016. Atlantic advection driven changes in glacial meltwater: Effects on phytoplankton chlorophyll-a and taxonomic composition in Kongsfjorden, Spitsbergen. Front. Mar. Sci. **3**. doi:10.3389/fmars.2016.00200

Wlodarska-Kowalczuk, M., and T. H. Pearson. 2004. Soft-bottom macrobenthic faunal associations and factors affecting species distributions in an Arctic glacial fjord (Kongsfjord, Spitsbergen). Polar Biol. **27**: 155–167. doi:10.1007/s00300-003-0568-y

Włodarska-Kowalczuk, M., B. Górska, K. Deja, and N. Morata. 2016. Do benthic meiofaunal and macrofaunal communities respond to seasonality in pelagial processes in an Arctic fjord (Kongsfjorden, Spitsbergen)? Polar Biol. **39**: 2115–2129. doi:10.1007/s00300-016-1982-2

Woehle, C., and others. 2022. Denitrification in foraminifera has an ancient origin and is complemented by associated bacteria. Proc. Natl. Acad. Sci. U. S. A. **119**: e2200198119. doi:10.1073/pnas.2200198119

Acknowledgments

We thank the Alfred Wegener Institute-Institute Paul Emile Victor (AWIPEV) station as well as King's Bay logistical staff for all the technical support provided before, during, and after the cruises and for the curation of CTD data. We furthermore thank the two captains of the MS *Teisten* who accompanied us during the sampling process. This work was supported by both the KONBHAS project (Kongsfjorden New Benthic HAbitatS; IPEV RIS 1223; project investigator: Professor Agnès Baltzer) for the campaigns funding and the BEGIN (Benthos under Arctic melting Glacier INfluence, LEFE CYBER CNRS, project investigator: Dr Maria Pia Nardelli) for the campaigns, analyses, and data curation funding. Additionally, we thank the other members of the KONBHAS project Hugues de Lauzon and Dr Francesca Caridi whose help was highly valuable on the field. We thank Anna R. Armitage for the editing process and Irina Polovodova Asteman and the 2 anonymous reviewers who helped to improve this manuscript.

Conflict of Interest

None declared.

Submitted 17 April 2024
Revised 12 July 2024
Accepted 30 August 2024

Associate Editor: Anna R. Armitage